

Multiple Testing of Local Extrema for Detection of Change Points *

Dan Cheng
North Carolina State University

Armin Schwartzman
North Carolina State University

April 21, 2021

Abstract

A new approach to change point detection based on smoothing and multiple testing is presented for long data sequences modeled as piecewise constant functions plus stationary ergodic Gaussian noise. As an application of the STEM algorithm for peak detection developed in Schwartzman et al. (2011) and Cheng & Schwartzman (2014), the method detects change points as significant local maxima and minima after smoothing and differentiating the observed sequence. The algorithm, combined with the Benjamini-Hochberg procedure for thresholding p-values, provides asymptotic strong control of the False Discovery Rate (FDR) and power consistency, as the length of the sequence and the size of the jumps get large. Simulations show that FDR levels are maintained in non-asymptotic conditions and guide the choice of smoothing bandwidth with respect to the desired location tolerance. The methods are illustrated in genomic array-CGH data.

Key Words: False discovery rate; Gaussian; Kernel smoothing; Local maxima; Local minima; Location tolerance.

1 Introduction

Detecting change points in the mean of an observed signal is a common statistical problem with applications in many research areas such as climatology (Reeves et al., 2007), oceanography (Killick et al., 2010), finance (Zeileis et al., 2010) and medical imaging (Nam et al., 2012). It often appears in the analysis of time series but it has more recently been found in the analysis of genomic sequences, see Erdman & Emerson (2008); Lai et al. (2005); Muggeo & Adelfio (2011); Olshen et al. (2004); Tibshirani & Wang (2008); Wang et al. (2005) and the references therein. Given the large amounts of data present in modern applications, it is of interest to design a change point detection method that

*Partially supported by NIH grant R01-CA157528.

can operate over long sequences where the number and location of change points are unknown, and in such a way that the overall detection error rate is controlled.

Many different approaches have been proposed to find and estimate change points, such as kernel-based methods (Gijbels, 2003), Bayesian methods (Barry & Hartigan, 1993; Erdman & Emerson, 2008), segmentation techniques (Olshen et al., 2004; Wang et al., 2005; Muggeo & Adelfio, 2011), nonparametric tests (Lanzante, 1996) and L_1 -penalty methods (Eilers & de Menezes, 2005; Huang et al., 2005; Tibshirani & Wang, 2008), including the PELT method (Jackson et al., 2005; Killick et al., 2012). However, the approach proposed here is unique in the following two ways.

First, the noise is assumed to be a stationary Gaussian process, allowing the error terms to be correlated. This is an important departure from the standard assumption of white noise in most of the change-point literature. In fact, applied statisticians desiring to use change-point methods have sometimes abandoned this option in favor of other techniques simply because the white noise assumption does not hold (Hung et al., 2013). This paper shows that change-point methods can be devised for correlated noise, expanding the domain of their applicability.

Second, we use the theory of Gaussian processes to compute p-values for all candidate change points, so that significant change points can be selected at a desired significance level. For concreteness, we adopt the Benjamini-Hochberg multiple testing procedure, enabling control of the false discovery rate (FDR) of detected change points when the data sequence is long and the number and location of change points are unknown. To our knowledge, this is the first article proposing a multiple testing method for controlling FDR of detected change points.

In this paper, we consider a signal-plus-noise model where the true signal is a piecewise constant function and the change points are defined as the points of discontinuity. Inspired by the method for detecting peaks in Schwartzman et al. (2011) and Cheng & Schwartzman (2014), we modify the STEM algorithm therein to detect change points. The central idea is the observation that the true signal has zero derivative everywhere except at the change points, where the derivative is infinite. Thus, in the presence of noise and under temporal or spatial sampling, change points can be seen as positive or negative peaks in the derivative of the smoothed signal. Note that because of the time sampling, derivatives cannot be observed directly and can only be estimated. The focus on the derivative of the smoothed signal effectively transforms the change point detection problem into a peak detection problem. As in the STEM algorithm, the resulting peak detection problem is then solved by identifying local maxima and minima of the derivative as candidate peaks and applying a multiple testing procedure to the list of candidates.

The modified STEM algorithm for change point detection consists of the following steps:

1. *Differential kernel smoothing*: to transform change points to local maxima or minima.
2. *Candidate peaks*: find local maxima and minima of the differentiated smoothed process.
3. *P-values*: computed at each local maximum and minimum under the the null hypothesis of no signal in a local neighborhood.

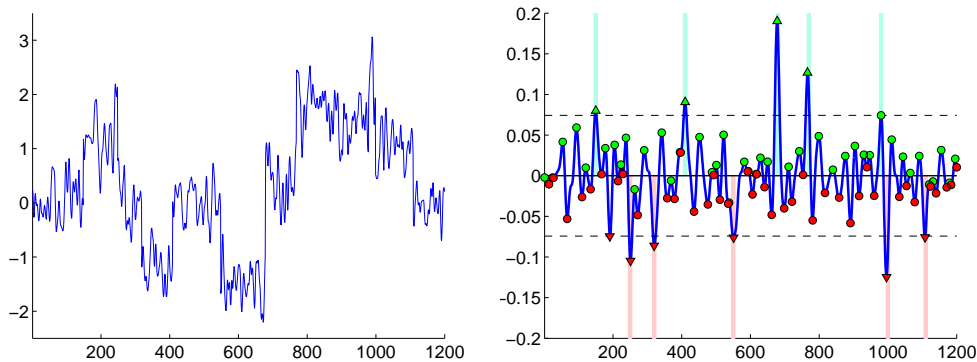


Figure 1: Following the notation in §2.1 and Example 3.4, the left panel is the observed signal-plus-noise model $y(t)$ containing ten true change points with varying a_i and noise $z(t)$ given by (3.5) with $\sigma = 1$ and $\nu = 2$. The right panel illustrates the STEM algorithm. The blue curve is $y'_\gamma(t)$, obtained with a Gaussian smoothing kernel with standard deviation $\gamma = 6$. Local maxima (green solid dots) and local minima (red solid dots) are declared as significant (marked with solid triangles) at FDR level $\alpha = 0.1$ if their heights are beyond the dotted line thresholds. The cyan and pink bars indicate the location tolerance intervals $(v_i - b, v_i + b)$ with $b = 5$ for increasing and decreasing change points respectively. At this tolerance, there are nine true discoveries and one false discovery.

4. *Multiple testing*: apply a multiple testing procedure to the set of local maxima and minima; declare as detected change points those local maxima and minima whose p-values are significant.

The algorithm is illustrated by a toy example in Figure 1.

The modified STEM algorithm above differs from the ones in Schwartzman et al. (2011) and Cheng & Schwartzman (2014) in that peaks are sought in the derivative of the smoothed signal rather than the smoothed signal itself, and that both positive and negative peaks are considered. In addition, an important consideration for the proper definition of error in change point detection is that, as opposed to the peak detection problems considered in Schwartzman et al. (2011) and Cheng & Schwartzman (2014) where signal peaks had compact support, a true single change point at $t = v$ has Lebesgue measure zero. Thus in the presence of noise, it can never be detected exactly at $t = v$. Therefore we introduce a *location tolerance* b that defines the precision within which a change point should be detected. Specifically, given b , a detected change point is regarded as a true discovery if it falls in the interval $(v - b, v + b)$. Conversely, if a significant change point is found more than a distance b from any true change point, it is considered a false discovery. The quantity b is not used in the STEM algorithm itself but is needed for proper error definition.

Under this convention, it is shown here that the modified STEM algorithm exhibits asymptotic FDR control and power consistency as the length of the sequence and the size of the jumps at the change points increase. These asymptotic conditions are similar to those considered in Schwartzman et al.

(2011) and Cheng & Schwartzman (2014) and, in fact, the proofs are easily extended from those in Cheng & Schwartzman (2014).

Simulations for varying levels of smoothing bandwidth γ , location tolerance b and jump size a are used to study the behavior of the algorithm under non-asymptotic conditions. The simulation results help guide the choice of smoothing bandwidth with respect to the desired location tolerance. In general, power increases with bandwidth to a limit dictated by the distance between the change points, so admitting a higher tolerance generally allows a higher bandwidth and higher power.

The methods are illustrated in a genomic sequence of array-CGH data in a breast-cancer tissue sample (Loo et al., 2005; Hsu et al., 2005). The goal of the analysis is to find genomic segments with copy-number alterations. These are found by detecting change points in the copy number genomic sequence.

2 The multiple testing scheme

2.1 The model

We consider a continuous time model, although the algorithm is designed for data discretely sampled in time. Consider the signal-plus-noise model

$$y(t) = \mu(t) + z(t), \quad t \in \mathbb{R}, \quad (2.1)$$

where the signal $\mu(t)$ is a piecewise constant function of the form

$$\mu(t) = \sum_{j=0}^{\infty} a_j h_j(t), \quad a_j \in \mathbb{R} \setminus \{0\},$$

with $h_j(t) = \mathbb{1}(t > v_j)$ for $v_j \in \mathbb{R}$. We are interested in finding the *change points* v_j . For the asymptotic analysis, we assume

$$a = \inf_j |a_j| > 0 \quad \text{and} \quad v = \inf_j |v_j - v_{j-1}| > 0,$$

so that the change points do not become arbitrarily small in size nor arbitrarily close to each other.

Let $w_\gamma(t) = w(t/\gamma)/\gamma$, where $\gamma > 0$ is the bandwidth parameter and $w(t) \geq 0$ is a unimodal symmetric kernel with compact connected support $[-c, c]$ and unit action. Convolution of the process (2.1) with the kernel $w_\gamma(t)$ results in the smoothed random process

$$y_\gamma(t) = w_\gamma(t) * y(t) = \int_{\mathbb{R}} w_\gamma(t-s)y(s) ds = \mu_\gamma(t) + z_\gamma(t), \quad (2.2)$$

where the smoothed signal and smoothed noise are defined respectively as

$$\mu_\gamma(t) = w_\gamma(t) * \mu(t) = \sum_{j=0}^{\infty} a_j h_{j,\gamma}(t) \quad \text{and} \quad z_\gamma(t) = w_\gamma(t) * z(t), \quad (2.3)$$

and where the smoothed change point takes the form

$$h_{j,\gamma}(t) = w_\gamma(t) * h_j(t). \quad (2.4)$$

The smoothed noise $z_\gamma(t)$ defined by (2.3) is assumed to be a zero-mean four-times differentiable stationary ergodic Gaussian process.

2.2 Change point detection as peak detection of the derivative

Consider now the derivative of the smoothed observed process (2.2)

$$y'_\gamma(t) = w'_\gamma(t) * y(t) = \int_{\mathbb{R}^N} w'_\gamma(t-s)y(s) ds = \mu'_\gamma(t) + z'_\gamma(t), \quad (2.5)$$

where the derivatives of the smoothed signal and smoothed noise are respectively

$$\mu'_\gamma(t) = w'_\gamma(t) * \mu(t) = \sum_{j=0}^{\infty} a_j h'_{j,\gamma}(t) \quad \text{and} \quad z'_\gamma(t) = w'_\gamma(t) * z(t).$$

A key observation from (2.4) is that

$$\begin{aligned} h'_{j,\gamma}(t) &= \int_{\mathbb{R}} w'_\gamma(t-s)h_j(s) ds = \int_{\mathbb{R}} w'_\gamma(s)h_j(t-s) ds \\ &= \int_{\mathbb{R}} w'_\gamma(s)\mathbb{1}(t-s > v_j) ds = w_\gamma(t-v_j). \end{aligned} \quad (2.6)$$

Thus (2.5) represents a signal-plus-noise model where the smoothed signal

$$\mu'_\gamma(t) = \sum_{j=0}^{\infty} a_j h'_{j,\gamma}(t) = \sum_{j=0}^{\infty} a_j w_\gamma(t-v_j) \quad (2.7)$$

is a sequence of unimodal peaks with the same shape as that of w_γ and located at locations v_j . The problem of finding change points in $y_\gamma(t)$ is thus reduced to finding (positive or negative) peaks in $y'_\gamma(t)$.

For simplicity, we assume that the compact supports $S_{j,\gamma}$ of the smoothed peak shape $h'_{j,\gamma}(t) = w_\gamma(t-v_j)$ do not overlap, although this is not crucial in practice.

2.3 The STEM algorithm for change point detection

Suppose we observe $y(t)$ with J jumps defined by (2.1) in the line of length L centered at the origin, denoted by $U(L) = (-L/2, L/2)$. The following is a version of the STEM algorithm of Schwartzman et al. (2011) and Cheng & Schwartzman (2014) for detecting change points.

Algorithm 2.1 (STEM algorithm for change point detection)

1. Differential kernel smoothing: Obtain the process (2.5) by convolution of $y(t)$ with the kernel derivative $w'_\gamma(t)$.

2. Candidate peaks: Find the set of local maxima and minima of $y'_\gamma(t)$ in $U(L)$, denoted by $\tilde{T}_\gamma = \tilde{T}_\gamma^+ \cup \tilde{T}_\gamma^-$, where

$$\begin{aligned}\tilde{T}_\gamma^+ &= \left\{ t \in U(L) : y''_\gamma(t) = 0, y_\gamma^{(3)}(t) < 0 \right\}, \\ \tilde{T}_\gamma^- &= \left\{ t \in U(L) : y''_\gamma(t) = 0, y_\gamma^{(3)}(t) > 0 \right\}.\end{aligned}$$

3. P-values: For each $t \in \tilde{T}_\gamma^+$, compute the p-value $p_\gamma(t)$ for testing the (conditional) hypotheses

$$\begin{aligned}\mathcal{H}_0(t) &: \{\mu'(s) = 0 \text{ for all } s \in (t-b, t+b)\} \text{ vs.} \\ \mathcal{H}_A(t) &: \{\mu'(s) > 0 \text{ for some } s \in (t-b, t+b)\};\end{aligned}$$

and for each $t \in \tilde{T}_\gamma^-$, compute the p-value $p_\gamma(t)$ for testing the (conditional) hypotheses

$$\begin{aligned}\mathcal{H}_0(t) &: \{\mu'(s) = 0 \text{ for all } s \in (t-b, t+b)\} \text{ vs.} \\ \mathcal{H}_A(t) &: \{\mu'(s) < 0 \text{ for some } s \in (t-b, t+b)\},\end{aligned}$$

where $b > 0$ is an appropriate location tolerance.

4. Multiple testing: Let $\tilde{m}_\gamma = \#\{t \in \tilde{T}_\gamma\}$ be the number of tested hypotheses. Apply a multiple testing procedure on the set of \tilde{m}_γ p-values $\{p_\gamma(t), t \in \tilde{T}_\gamma\}$, and declare significant all local extrema whose p-values are smaller than the significance threshold.

2.4 P-values

Given the observed heights $y'_\gamma(t)$ at the local maxima or minima $t \in \tilde{T}_\gamma = \tilde{T}_\gamma^+ \cup \tilde{T}_\gamma^-$, p-values in step (3) of Algorithm 2.1 are computed as

$$p_\gamma(t) = \begin{cases} F_\gamma(y'_\gamma(t)), & t \in \tilde{T}_\gamma^+, \\ F_\gamma(-y'_\gamma(t)), & t \in \tilde{T}_\gamma^-, \end{cases} \quad (2.8)$$

where $F_\gamma(u)$ denotes the right tail probability of $z'_\gamma(t)$ at the local maximum $t \in \tilde{T}_\gamma^+$, evaluated under the null model $\mu'(s) = 0, \forall s \in (t-b, t+b)$, that is,

$$F_\gamma(u) = \mathbb{P}(z'_\gamma(t) > u \mid t \text{ is a local maximum of } z'_\gamma(t)). \quad (2.9)$$

The second line in (2.8) is obtained by noting that, by (2.9),

$$\begin{aligned}\mathbb{P}(z'_\gamma(t) < u \mid t \text{ is a local minimum of } z'_\gamma(t)) \\ = \mathbb{P}(-z'_\gamma(t) > -u \mid t \text{ is a local maximum of } -z'_\gamma(t)) = F_\gamma(-u),\end{aligned}$$

since $-z'_\gamma(t)$ and $z'_\gamma(t)$ have the same distribution.

The distribution (2.9) has a closed-form expression, which can be obtained as in Schwartzman et al. (2011) or Cramér & Leadbetter (1967). More specifically, the distribution (2.9) is given by

$$F_\gamma(u) = 1 - \Phi\left(u\sqrt{\frac{\lambda_{6,\gamma}}{\Delta}}\right) + \sqrt{\frac{2\pi\lambda_{4,\gamma}^2}{\lambda_{6,\gamma}\sigma_\gamma'^2}}\phi\left(\frac{u}{\sigma_\gamma'}\right)\Phi\left(u\sqrt{\frac{\lambda_{4,\gamma}^2}{\Delta\sigma_\gamma'^2}}\right), \quad (2.10)$$

where $\sigma_\gamma'^2 = \text{Var}(z_\gamma'(t))$, $\lambda_{4,\gamma} = \text{Var}(z_\gamma''(t))$, $\lambda_{6,\gamma} = \text{Var}(z_\gamma^{(3)}(t))$, $\Delta = \sigma_\gamma'^2\lambda_{6,\gamma} - \lambda_{4,\gamma}^2$, and $\phi(x)$, $\Phi(x)$ are the standard normal density and cumulative distribution function, respectively. The quantities $\sigma_\gamma'^2$, $\lambda_{4,\gamma}$ and $\lambda_{6,\gamma}$ depend on the kernel $w_\gamma(t)$ and the autocorrelation function of the original noise process $z(t)$. Explicit expressions may be obtained, for instance, for the Gaussian autocorrelation model in Example 3.4 below, which we use later in the simulations.

2.5 Error definitions

Assuming the model of §2.1, define the *signal region* $\mathbb{S}_1^b = \cup_{j=1}^J(v_j - b, v_j + b)$ and *null region* $\mathbb{S}_0^b = U(L) \setminus \mathbb{S}_1^b$. For $u > 0$, let $\tilde{T}_\gamma(u) = \tilde{T}_\gamma^+(u) \cup \tilde{T}_\gamma^-(u)$, where

$$\begin{aligned} \tilde{T}_\gamma^+(u) &= \left\{t \in U(L) : y_\gamma'(t) > u, y_\gamma''(t) = 0, y_\gamma^{(3)}(t) < 0\right\}, \\ \tilde{T}_\gamma^-(u) &= \left\{t \in U(L) : y_\gamma'(t) < -u, y_\gamma''(t) = 0, y_\gamma^{(3)}(t) > 0\right\}, \end{aligned}$$

indicating that $\tilde{T}_\gamma^+(u)$ and $\tilde{T}_\gamma^-(u)$ are respectively the set of local maxima of $y_\gamma'(t)$ above u and the set of local minima of $y_\gamma'(t)$ below $-u$. The number of totally and falsely detected change points at threshold u are defined respectively as

$$\begin{aligned} R_\gamma(u) &= \#\{t \in \tilde{T}_\gamma^+(u)\} + \#\{t \in \tilde{T}_\gamma^-(u)\}, \\ V_\gamma(u; b) &= \#\{t \in \tilde{T}_\gamma^+(u) \cap \mathbb{S}_0^b\} + \#\{t \in \tilde{T}_\gamma^-(u) \cap \mathbb{S}_0^b\}. \end{aligned} \quad (2.11)$$

Both are defined as zero if $\tilde{T}_\gamma(u)$ is empty. The FDR at threshold u is defined as the expected proportion of falsely detected jumps

$$\text{FDR}_\gamma(u; b) = \mathbb{E} \left\{ \frac{V_\gamma(u; b)}{R_\gamma(u) \vee 1} \right\}. \quad (2.12)$$

Note that when γ and u are fixed, $V_\gamma(u; b)$ and hence $\text{FDR}_\gamma(u; b)$ are decreasing in b .

Following the notation in Cheng & Schwartzman (2014), define the *smoothed signal region* $\mathbb{S}_{1,\gamma}$ to be the support of $\mu_\gamma'(t)$ and *smoothed null region* $\mathbb{S}_{0,\gamma} = U(L) \setminus \mathbb{S}_{1,\gamma}$. We call the difference between the expanded signal support due to smoothing and the true signal support the *transition region* $\mathbb{T}_\gamma = \mathbb{S}_{1,\gamma} \setminus \mathbb{S}_1^b = \mathbb{S}_0^b \setminus \mathbb{S}_{0,\gamma}$.

2.6 Power

Denote by I^+ and I^- the collections of indices j corresponding to increasing and decreasing change points v_j , respectively. We define the power of Algorithm 2.1 as the expected fraction of true discov-

ered change points

$$\begin{aligned} \text{Power}_\gamma(u; b) = \frac{1}{J} \sum_{j=1}^J \text{Power}_{j,\gamma}(u; b) = \mathbb{E} \left[\frac{1}{J} \left(\sum_{j \in I^+} \mathbb{1} \left(\tilde{T}_\gamma^+(u) \cap (v_j - b, v_j + b) \neq \emptyset \right) \right. \right. \\ \left. \left. + \sum_{j \in I^-} \mathbb{1} \left(\tilde{T}_\gamma^-(u) \cap (v_j - b, v_j + b) \neq \emptyset \right) \right) \right], \end{aligned} \quad (2.13)$$

where $\text{Power}_{j,\gamma}(u; b)$ is the probability of detecting jump v_j within a distance b ,

$$\text{Power}_{j,\gamma}(u; b) = \begin{cases} \mathbb{P} \left(\tilde{T}_\gamma^+(u) \cap (v_j - b, v_j + b) \neq \emptyset \right), & \text{if } j \in I^+, \\ \mathbb{P} \left(\tilde{T}_\gamma^-(u) \cap (v_j - b, v_j + b) \neq \emptyset \right), & \text{if } j \in I^-. \end{cases} \quad (2.14)$$

The indicator function in (2.13) ensures that only one significant local extremum is counted within a distance b of a change point, so power is not inflated. Note that when γ and u are fixed, $\text{Power}_\gamma(u; b)$ and $\text{Power}_{j,\gamma}(u; b)$ are increasing in b .

3 Asymptotic error control and power consistency

Suppose the BH procedure is applied in step 4 of Algorithm 2.1 as follows. For a fixed $\alpha \in (0, 1)$, let k be the largest index for which the i th smallest p-value is less than $i\alpha/\tilde{m}_\gamma$. Then the null hypothesis $\mathcal{H}_0(t)$ at $t \in \tilde{T}_\gamma$ is rejected if

$$p_\gamma(t) < \frac{k\alpha}{\tilde{m}_\gamma} \iff \begin{cases} y'_\gamma(t) > \tilde{u}_{\text{BH}} = F_\gamma^{-1} \left(\frac{k\alpha}{\tilde{m}_\gamma} \right) & \text{if } t \in \tilde{T}_\gamma^+, \\ y'_\gamma(t) < -\tilde{u}_{\text{BH}} = -F_\gamma^{-1} \left(\frac{k\alpha}{\tilde{m}_\gamma} \right) & \text{if } t \in \tilde{T}_\gamma^-, \end{cases} \quad (3.1)$$

where $k\alpha/\tilde{m}_\gamma$ is defined as 1 if $\tilde{m}_\gamma = 0$. Since \tilde{u}_{BH} is random, we define FDR in such BH procedure as

$$\text{FDR}_{\text{BH},\gamma}(b) = \mathbb{E} \left\{ \frac{V_\gamma(\tilde{u}_{\text{BH}}; b)}{R_\gamma(\tilde{u}_{\text{BH}}) \vee 1} \right\},$$

where $R_\gamma(\cdot)$ and $V_\gamma(\cdot; b)$ are defined in (2.11) and the expectation is taken over all possible realizations of the random threshold \tilde{u}_{BH} . We will make use of the following conditions:

(C1) The assumptions of §2.1 hold.

(C2) $L \rightarrow \infty$ and $a = \inf_j |a_j| \rightarrow \infty$, such that $(\log L)/a^2 \rightarrow 0$, $J/L = A_1 + O(a^{-2} + L^{-1/2})$ with $A_1 > 0$.

Let $\mathbb{E}[\tilde{m}_{0,\gamma}(U(1))]$ and $\mathbb{E}[\tilde{m}_{0,\gamma}(U(1), u)]$ be the expected number of local maxima and local maxima above level u of $z'_\gamma(t)$ on unit interval $U(1) = (-1/2, 1/2)$, respectively. In particular, we have the following explicit formula (Schwartzman et al., 2011)

$$\mathbb{E}[\tilde{m}_{0,\gamma}(U(1))] = \frac{1}{2\pi} \sqrt{\frac{\lambda_{6,\gamma}}{\lambda_{4,\gamma}}}. \quad (3.2)$$

Theorem 3.1 *Let conditions (C1) and (C2) hold.*

(i) *Suppose Algorithm 2.1 is applied with a fixed threshold $u > 0$. Then*

$$\text{FDR}_\gamma(u; b) \leq \frac{2\mathbb{E}[\tilde{m}_{0,\gamma}(U(1), u)](1 - 2c\gamma A_1)}{2\mathbb{E}[\tilde{m}_{0,\gamma}(U(1), u)](1 - 2c\gamma A_1) + A_1} + O(a^{-2} + L^{-1/2}).$$

(ii) *Suppose Algorithm 2.1 is applied with the random threshold \tilde{u}_{BH} (3.1). Then*

$$\text{FDR}_{\text{BH},\gamma}(b) \leq \alpha \frac{2\mathbb{E}[\tilde{m}_{0,\gamma}(U(1))](1 - 2c\gamma A_1)}{2\mathbb{E}[\tilde{m}_{0,\gamma}(U(1))](1 - 2c\gamma A_1) + A_1} + O(a^{-1} + L^{-1/4}).$$

Proof Since $w_\gamma(t)$ has compact support $[-c\gamma, c\gamma]$, by (2.6), the support $\mathbb{S}_{1,\gamma}$ of $\mu'_\gamma(t)$ in (2.7) is composed of the support segments $[v_j - c\gamma, v_j + c\gamma]$ of $h'_{j,\gamma}(t)$. By condition (C2), $|\mathbb{S}_{1,\gamma}|/L = 2c\gamma A_1 + O(a^{-2} + L^{-1/2})$, which implies $|\mathbb{S}_{0,\gamma}|/L = 1 - 2c\gamma A_1 + O(a^{-2} + L^{-1/2})$.

Notice that, on the null region $\mathbb{S}_{0,\gamma}$, the expected number of local extrema, including both local maxima and minima, equals $2|\mathbb{S}_{0,\gamma}|\mathbb{E}[\tilde{m}_{0,\gamma}(U(1))]$. On the other hand, similarly to the proof of Theorem 3 in Cheng & Schwartzman (2014), the expected number of local extrema on the signal region $\mathbb{S}_{1,\gamma}$ is asymptotically equivalent to J . This is because, for each $j \in I^+$ and $b > 0$, as $a \rightarrow \infty$, asymptotically, there is no local maximum of $y'_\gamma(t)$ in $(v_j - c\gamma, v_j - b) \cup (v_j + b, v_j + c\gamma)$, and there is only one local maximum of $y'_\gamma(t)$ in $(v_j - b, v_j + b)$.

The result then follows from similar arguments for proving Theorem 3 in Cheng & Schwartzman (2014) with $N = 1$, $A_{2,\gamma} = 2c\gamma A_1$, $z_\gamma(t)$ replaced by $z'_\gamma(t)$ and $\mathbb{E}[\tilde{m}_{0,\gamma}(U(1))]$ replaced by $2\mathbb{E}[\tilde{m}_{0,\gamma}(U(1))]$. \square

Lemma 3.2 *Let conditions (C1) and (C2) hold. As $|a_j| \rightarrow \infty$, the power for peak j and fixed u (2.14) can be approximated by*

$$\text{Power}_{j,\gamma}(u; b) = \Phi\left(\frac{|a_j|w_\gamma(0) - u}{\sigma'_\gamma}\right) (1 + O(|a_j|^{-2})). \quad (3.3)$$

Proof By (2.6), $h'_{j,\gamma}(v_j) = w_\gamma(0)$ is the maximum of $h'_{j,\gamma}(t)$ over $t \in \mathbb{R}$. The result then follows from similar arguments for proving Lemma 4 in Cheng & Schwartzman (2014) with $z_\gamma(t)$ replaced by $z'_\gamma(t)$. \square

By similar arguments in Cheng & Schwartzman (2014) (see equation (20) therein), one can show that the random threshold \tilde{u}_{BH} converges asymptotically to the deterministic threshold

$$u_{\text{BH}}^* = F_\gamma^{-1}\left(\frac{\alpha A_1}{A_1 + 2\mathbb{E}[\tilde{m}_{0,\gamma}(U(1))](1 - 2c\gamma A_1)(1 - \alpha)}\right), \quad (3.4)$$

where $E[\tilde{m}_{0,\gamma}(U(1))]$ is given by (3.2). Since \tilde{u}_{BH} is random, similarly to the definition of $\text{FDR}_{\text{BH},\gamma}(b)$, we define power in the BH procedure as

$$\text{Power}_{\text{BH},\gamma}(b) = E \left[\frac{1}{J} \left(\sum_{j \in I^+} \mathbb{1} \left(\tilde{T}_\gamma^+(\tilde{u}_{\text{BH}}) \cap (v_j - b, v_j + b) \neq \emptyset \right) + \sum_{j \in I^-} \mathbb{1} \left(\tilde{T}_\gamma^-(\tilde{u}_{\text{BH}}) \cap (v_j - b, v_j + b) \neq \emptyset \right) \right) \right].$$

Theorem 3.3 *Let conditions (C1) and (C2) hold.*

(i) *Suppose Algorithm 2.1 is applied with a fixed threshold $u > 0$. Then*

$$\text{Power}_\gamma(u; b) = 1 - O(a^{-2}).$$

(ii) *Suppose Algorithm 2.1 is applied with the random threshold \tilde{u}_{BH} (3.1). Then*

$$\text{Power}_{\text{BH},\gamma}(b) = 1 - O(a^{-2} + L^{-1/2}).$$

Proof The desired results follow from similar arguments for showing Theorem 5 in Cheng & Schwartzman (2014). \square

Example 3.4 [Gaussian autocorrelation model] Let the noise $z(t)$ in (2.1) be constructed as

$$z(t) = \sigma \int_{\mathbb{R}} \frac{1}{\nu} \phi \left(\frac{t-s}{\nu} \right) dB(s), \quad \sigma, \nu > 0, \quad (3.5)$$

where ϕ is the standard Gaussian density, $dB(s)$ is Gaussian white noise and $\nu > 0$ ($z(t)$ is regarded by convention as Gaussian white noise when $\nu = 0$). Convolving with a Gaussian kernel $w_\gamma(t) = (1/\gamma)\phi(t/\gamma)$ with $\gamma > 0$ as in (2.3) produces a zero-mean infinitely differentiable stationary ergodic Gaussian field $z_\gamma(t)$ such that

$$z'_\gamma(t) = w'_\gamma(t) * z(t) = \sigma \int_{\mathbb{R}^N} \frac{-(t-s)}{\xi^2} \phi \left(\frac{t-s}{\xi} \right) dB(s), \quad \xi = \sqrt{\gamma^2 + \nu^2},$$

with $\sigma_\gamma'^2 = \sigma^2/(4\sqrt{\pi}\xi^3)$, $\lambda_{4,\gamma} = 3\sigma^2/(8\sqrt{\pi}\xi^5)$ and $\lambda_{6,\gamma} = 33\sigma^2/(16\sqrt{\pi}\xi^7)$. We have

$$\text{SNR}_{j,\gamma} = \frac{a_j w_\gamma(0)}{\sigma'_\gamma} = \frac{\sqrt{2}|a_j|}{\sigma\pi^{1/4}} \left[\frac{(\gamma^2 + \nu^2)^{3/4}}{\gamma} \right]. \quad (3.6)$$

As a function of γ , the SNR has a local minimum at $\gamma^* = \sqrt{2}\nu$ and is strictly increasing for large γ . In particular, when $\nu = 0$, it is strictly increasing in γ . Thus we generally expect the detection power to increase with γ for $\gamma > \sqrt{2}\nu$. This will be confirmed in the simulations below. Note that for $\nu > 0$, the SNR is unbounded as $\gamma \rightarrow 0$, however in practice γ cannot be too small: if the support of w_γ becomes smaller than the sampling interval, then the derivative μ'_γ cannot be estimated.

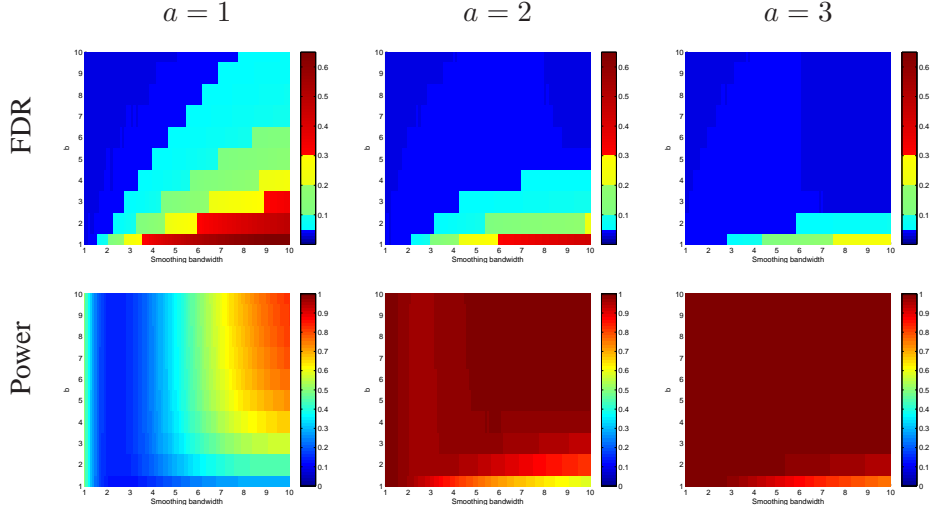


Figure 2: Realized FDR and power of the BH procedure for $d = 100$.

4 Simulation studies

Simulations were used to evaluate the performance and limitations of the STEM algorithm for signals $\mu(t) = a\lfloor t/d \rfloor$, where $t = 1, \dots, L$, $L = 12000$, $d \in \{100, 15\}$ and signal strength $a \in \{1, 2, 3\}$. Under this setting, the true change points are $v_j = jd$ for $j = 1, \dots, L/d - 1$. The noise is generated as the Gaussian process constructed in (3.5) with $\sigma = 1$ and $\nu = 2$. The smoothing kernels are $w_\gamma(t) = (1/\gamma)\phi(t/\gamma)\mathbb{1}(t \in [-4\gamma, 4\gamma])$ for varying γ . The BH procedure was applied at FDR level $\alpha = 0.05$. Results were averaged over 10,000 replications to simulate the expectations.

Figure 2 shows the realized FDR and detection power for a change point separation of $d = 100$. A special color map was used for FDR to emphasize the control of FDR (FDR values less than the nominal level 0.05 appear in dark blue). We see that for every fixed bandwidth γ , increasing the location tolerance b allows for detections to be counted as true farther away from the true change points, thereby decreasing FDR and increasing power. On the other hand, as expected from Theorems 3.1 and 3.3, as the strength of the signal a increases, FDR is eventually controlled below the nominal level and the power tends to 1 for every combination of parameters γ and b .

For a fixed tolerance b , increasing the bandwidth γ increases FDR by moving some true change points beyond b and producing artificial errors. This also results in some loss of power, which can be seen in Figure 2 especially when b is small and γ is large. In addition, for larger b and smaller γ , the power is seen to first decrease quickly and then increase again as γ increases. This phenomenon coincides with the behavior of the SNR (3.6) derived in Example 3.4, predicting the power to decrease for $\gamma \leq \sqrt{2\nu}$ and increase for $\gamma > \sqrt{2\nu}$.

Figure 3 illustrates this phenomenon more clearly for fixed $b = 8$. The realized FDR curves have the same shape as the “theoretical power” curves, obtained by plugging the asymptotic threshold u_{BH}^*

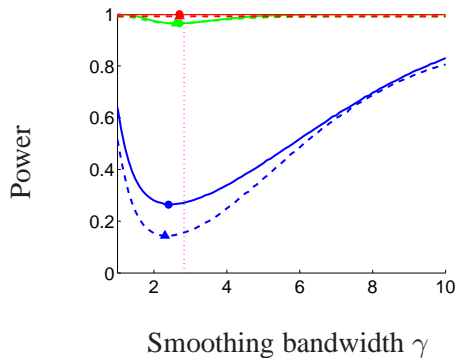


Figure 3: The solid curves and dotted curves (in both cases, blue for $a = 1$, green for $a = 2$ and red for $a = 3$) are respectively “theoretical powers” and realized powers from Figure 2 with $b = 8$. The pink dotted vertical line is $\gamma = \sqrt{2}\nu$ as shown in Example 3.4.

(3.4) into the approximate power (3.3). Both curves get closer to 1 as the signal strength a increases.

The separation of $d = 100$ in Figure 2 is large enough that bandwidths up to $\gamma = 10$ do not produce any interference between neighboring change points. To investigate the effect of neighboring interference, Figure 4 shows the realized FDR and detection power for a change point separation of $d = 15$. It can be seen that increasing γ beyond 5 will produce interference and contamination error, thereby decreasing power. Still, for any fixed γ and b , FDR will eventually be controlled and power will increase if the signal strength is large enough.

5 Data example

5.1 Data description

Array-based comparative genomic hybridization (array-CGH) is a high-throughput high-resolution technique used to evaluate changes in the number of copies of alleles at thousands of genomic loci simultaneously. The output is often called Copy Number Variation (CNV) data. Changes in copy number are represented by segments whose mean is displaced with respect to the background. To detect these changes, it is customary to search for change points along the genome.

In this paper, we apply our method to chromosome 1 of tumor sample #18 from the dataset of Hsu et al. (2005) and Loo et al. (2005). This sample is one of 37 formalin-fixed breast cancer tumors in that dataset and it was chosen for its visual appeal in the illustration of our method. The data in chromosome 1 of tumor sample #18 consists of 968 average copy number reads mapped onto 968 unequally spaced locations along the chromosome. For simplicity, the data was analyzed ignoring the gaps in the genomic locations: Figure 5 (top left) shows the data with spacings between reads artificially set to 1. Note that ignoring the spacings does not affect the presence or absence of change points.

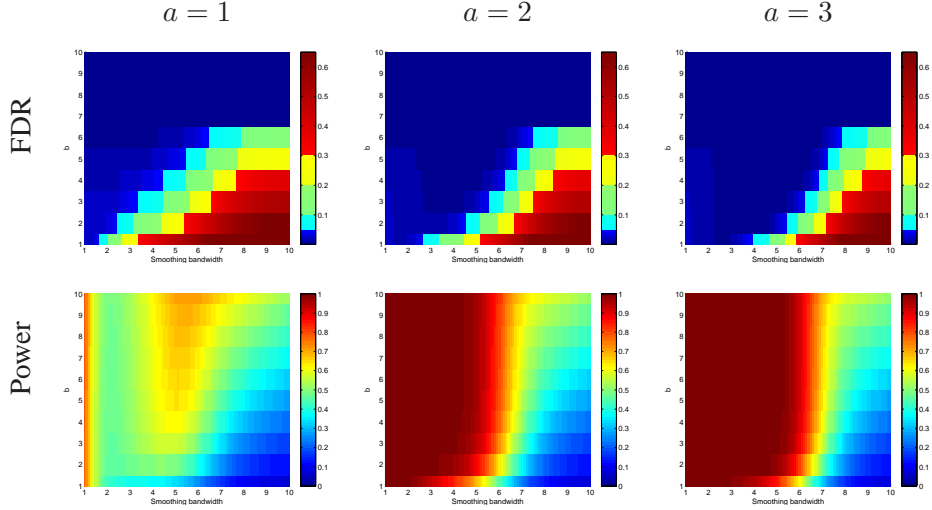


Figure 4: Realized FDR and power of the BH procedure for $d = 15$.

5.2 Data analysis

To analyze the data, the STEM algorithm was applied with a truncated Gaussian smoothing kernel $w_\gamma(t) = (1/\gamma)\phi(t/\gamma)\mathbb{1}(t \in [-4\gamma, 4\gamma])$ with $\gamma = 10$. The bandwidth was chosen not too large in order to avoid interference between neighboring change points. Figure 5 (top right) shows the estimated first derivative (2.5). Figure 5 (bottom left) marks 19 local maxima (green) and 19 local minima (red).

P-values corresponding to local maxima and minima were computed according to (2.8) using the distribution (2.10). The required parameters $\sigma_\gamma'^2 = \text{Var}(z_\gamma'(t))$, $\lambda_{4,\gamma} = \text{Var}(z_\gamma''(t))$, $\lambda_{6,\gamma} = \text{Var}(z_\gamma^{(3)}(t))$ were estimated empirically from the estimated first, second and third derivatives over the observed data sequence. However, the empirical variances were computed using truncated averages instead of regular averages in order to avoid bias from the extreme derivatives at the change points without assuming their presence or location in advance. The BH algorithm was applied to the 38 p-values FDR level 0.2, yielding a p-value significance threshold of 4.42×10^{-4} . The corresponding absolute height threshold of 0.089 is marked as dashed lines in Figure 5 (bottom left). The significant peaks are plotted on the original data in Figure 5 (bottom right) with a location tolerance of $b = 2$ for visual reference.

6 Discussion

In this paper, we combined both local maxima and minima as candidate peaks, and then applied a multiple testing procedure to find a uniform threshold (in absolute value) for detecting all change points. This approach is sensible when the distributions (number and height) of true increasing and

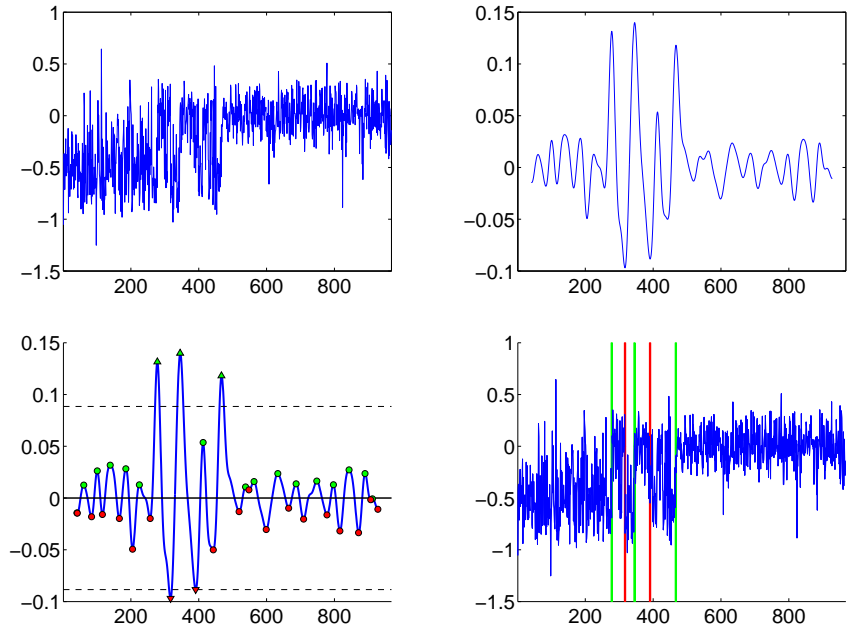


Figure 5: Data example. Top left: Observed data. Top right: estimated first derivative. Bottom left: local maxima (upward triangles), local minima (downward triangles) of the estimated first derivative, and significance height threshold (black dashed). Bottom right: The detected positive (green) and negative (red) change points.

decreasing change points are about the same. Alternatively, different thresholds for detecting increasing and decreasing change points could be found by applying separate multiple testing procedures to the sets of candidate local maxima and local minima. While we applied the BH algorithm to control FDR, in principle other multiple testing procedures may be used to control other error rates.

A natural and important question is how to choose the smoothing bandwidth γ . From Example 3.4 and Figures 2 and 4, we see that either a very small γ or a relatively large γ is preferred in order to increase power, but only to the extent that the smoothed signal supports $h'_{j,\gamma}(t)$ have little overlap and that detected change points are not displaced by more than the desired tolerance b (recall that the value of b is not used in the STEM algorithm itself, but it may be determined by the needs of the specific scientific application). Considering the Gaussian kernel to have an effective support of $\pm c\gamma$, a good value of γ may be about $\min(b, d/c)$, where d is the separation between change points. Since the location of the change points is unknown, a more precise optimization of γ may require an iterative procedure. Moreover, if some change points are close together and others are far apart, an adaptive bandwidth may be preferable. We leave these as problems for future research.

References

- ADLER, R. J. & TAYLOR, J. E. (2007). *Random Fields and Geometry*. Springer, New York.
- BARRY, D. & HARTIGAN, J. A. (1993). A Bayesian analysis for change point problems. *J. Am. Statist. Assoc.* **88**, 309–319.
- BENJAMINI, Y. & HOCHBERG, Y. (1995). Controlling the false discovery rate: a practical and powerful approach to multiple testing. *J. R. Statist. Soc. B* **57**, 289–300.
- CHENG, D. & SCHWARTZMAN, A. (2014a). Distribution of the height of local maxima of Gaussian random fields. *Extremes*, to appear. arXiv:1307.5863
- CHENG, D. & SCHWARTZMAN, A. (2014b). Multiple testing of local maxima for detection of peaks in random fields. arXiv:1405.1400
- CRAMÉR, H. & LEADBETTER, M. R. (1967). *Stationary and Related Stochastic Processes*. Wiley, New York.
- EILERS, P. H. C. & DE MENEZES, R. X. (2005). Quantile smoothing of array CGH data. *Bioinformatics* **21**, 1146–1153.
- ERDMAN, C. & EMERSON J. W. (2008). A fast Bayesian change point analysis for the segmentation of microarray data. *Bioinformatics* **24**, 2143–2148.
- GIJBELS, I. (2003). Inference for nonsmooth regression curves and surfaces using kernel-based methods. *a survey collected in “Recent advances and trends in nonparametric statistics” by Michael G. Akritas and Dimitris N. Politis*.
- HUANG, T., WU, B., LIZARDI, P. & ZHAO, H. (2005). Detection of DNA copy number alterations using penalized least squares regression. *Bioinformatics* **21**, 3811–3817.
- HUNG, Y., WANG, Y., ZARNITSYNA, V., ZHU, C. & WU C. F. J. (2013). Hidden Markov models with applications in cell adhesion experiments. *J. Am. Statist. Assoc.* **108**, 1469–1479.
- HSU, L., SELF, S. G., GROVE, D., RANDOLPH, T., WANG, K., DELROW, J. J., LOO, L. & PORTER, P. (2005). Denoising array-based comparative genomic hybridization data using wavelets. *Biostatistics* **6**, 211–226.
- JACKSON, B., SCARGLE, J. D., BARNES, D., ARABHI, S., ALT, A., GIOUMOUSIS, P., GWIN, E., SANG-TRAKULCHAROEN, P., TAN, L. & TSAI, T. T. (2005). An Algorithm for Optimal Partitioning of Data on an Interval. *IEEE, Signal Processing Letters* **12**, 105–108.
- KILLICK, R., ECKLEY, I. A., EWANS, K. & JONATHAN, P. (2010). Detection of changes in variance of oceanographic time-series using changepoint analysis. *Ocean Engineering* **37**, 1120–1126.
- KILLICK, R., FEARNHEAD, P. & ECKLEY, I. A. (2012). Optimal detection of changepoints with a linear computational cost. *J. Am. Statist. Assoc.* **107**, 1590–1598.
- LAI, W. R., JOHNSON, M. D., KUCHERLAPATI, R. & PARK, P. J. (2005). Comparative analysis of algorithms for identifying amplifications and deletions in array CGH data. *Bioinformatics* **21**, 3763–3770.

- LOO, L. W. M., GROVE, D. I., NEAL, C. L., COUSENS, L. A., SCHUBERT, E. L., WILLIAMS, E. M., HOLCOMB, I. N., DELROW, J. J., TRASK, B. J., HSU, L. & PORTER, P. L. (2004). Array-CGH analysis of genomic alterations in breast cancer subtypes. *Cancer Research* **64**, 8541–8549.
- LANZANTE, J. R. (1996). Resistant, robust and non-parametric techniques for the analysis of climate data: Theory and example, including applications to historical radiosonde station data. *International Journal of Climatology* **16**, 1197–1226.
- MUGGEO, V. M. R. & ADELFIGIO, G. (2011). Efficient change point detection for genomic sequences of continuous measurements. *Bioinformatics* **27**, 161–166.
- NAM, C. F. H., ASTON, J. A. D. & JOHANSEN, A. M. (2012). Quantifying the uncertainty in change points. *Journal of Time Series Analysis* **33**, 807–823.
- OLSHEN, A. B., VENKATRAMAN, E. S., LUCITO, R. & WIGLER, M. (2004). Circular binary segmentation for the analysis of array-based DNA copy number data. *Biostatistics* **5**, 557–572.
- REEVES, J., CHEN, J., WANG, X. L., LUND, R. & LU, Q. Q. (2007). A Review and Comparison of Change-point Detection Techniques for Climate Data. *Journal of Applied Meteorology and Climatology* **46**, 900–915.
- SCHWARTZMAN, A., DOUGHERTY, R. F. & TAYLOR, J. E. (2008). False discovery rate analysis of brain diffusion direction maps. *Ann. Appl. Statist.* **2**, 153–175.
- SCHWARTZMAN, A., GAVRILOV, Y. & ADLER, R. J. (2011). Multiple testing of local maxima for detection of peaks in 1D. *Ann. Statist.* **39**, 3290–3319.
- TIBSHIRANI, R. & WANG, P. (2008). Spatial smoothing and hot spot detection for CGH data using the fused lasso. *Biostatistics* **9**, 18–29.
- WANG, P., KIM, Y., POLLACK, J., NARASIMHAN, B. & TIBSHIRANI, R. (2005). A method for calling gains and losses in array CGH data. *Biostatistics* **6**, 45–58.
- ZEILEIS, A., SHAH, A. & PATNAIK, I. (2010). Testing, Monitoring, and Dating Structural Changes in Exchange Rate Regimes. *Computational Statistics & Data Analysis* **54**, 1696–1706.